# Theoretical *ab initio* study of the electronic states of KrH and $KrH^+$: Quantum defect and complex coordinate calculations on the Rydberg states of KrH

Ioannis D. Petsalakis and Giannoula Theodorakopoulos
*Theoretical and Physical Chemistry Institute, The National Hellenic Research Foundation, 48 Vassileos Constantinou Avenue, Athens 116 35, Greece*

Robert J. Buenker
*Bergische Universitaet Wuppertal, Fachbereich 9, Theoretische Chemie, Gaussstrasse 20, D-42097 Wuppertal, Germany*

(Received 12 March 2003; accepted 24 April 2003)

Potential energy curves have been calculated for the ground and excited electronic states of KrH and the cation $KrH^+$ by *ab initio* configuration interaction calculations using effective core potentials for Kr. Quantum defect functions have been determined from the *ab initio* potentials of the low-lying Rydberg states of KrH and potential energy curves have been generated for higher $n$ $(s,p,d)$ Rydberg states. The resulting bound–bound transition energies are in excellent agreement with experimental data. The interaction of the $5p$ $B\,^2\Pi$ state with the $5s$ and $5p$ $A\,^2\Sigma$ and $C\,^2\Sigma^+$ states and their predissociation by $X\,^2\Sigma^+$ has been treated by multistate complex scaling calculations for both KrH and KrD. Much larger predissociation widths are obtained in KrH than in KrD, in agreement with experimental observations. © *2003 American Institute of Physics.*
[DOI: 10.1063/1.1582837]

## I. INTRODUCTION

There is continuing interest in the Rydberg spectra of diatomic rare-gas hydrides,[1,2] since the first observation of the Rydberg spectra of ArH.[3] With a single electron outside a stable closed-shell cation core, these systems have repulsive ground electronic states with only shallow van der Waals minima and stacks of bound Rydberg states[4] and for this reason they are also called Rydberg molecules.[5] This typical picture of the potential energy curves of the electronic states of rare-gas hydrides was also found for KrH which is the system of interest in the present work. *Ab initio* calculations[6] showed that the ground state of KrH is repulsive and it is the lower state in the observed bound-repulsive spectra of this system,[7] while the corresponding lower state for the bound to bound Rydberg spectra is the first excited state of KrH, $A\,^2\Sigma^+$. The possibility that the ground state was the lower state of the observed bound–bound spectra had been originally proposed[5,8] but in subsequent work the $A\,^2\Sigma^+$ state was given as the lowest bound state of KrD, in agreement with the *ab initio* calculations.[6] The first bound–bound Rydberg spectra of KrH and KrD were reported in 1988 by Dabrowski *et al.*[8] where an analysis of the observed spectra by analogy of the observed levels with the spectrum of Rb gave reasonable assignments but could not account for observed bands at 5200 $cm^{-1}$.[8] In more recent work by Dabrowski and Sadowski[9] additional emission bands of KrD were analyzed and the series previously labeled as $nd$ $(^2\Sigma^+, ^2\Pi, ^2\Delta)$ was recognized as the Rydberg series of $np$ complexes while the previously assigned $np\,^2\Pi \rightarrow A\,^2\Sigma^+$ bands[8] were assigned as $nd\,^2\Pi \rightarrow A\,^2\Sigma^+$.

It is possible to assign many of the observed bands in the spectra of rare-gas hydrides in terms of case (b) states, e.g., $^2\Sigma^+$, $^2\Pi$. However, in other cases as, for example, bands arising from the $np$ and the $nf$ states of KrD[9,10] and also of ArH and ArD,[11] it is necessary to describe these states in terms of case (d) $l$-complexes in order to explain the rotational structure of the observed spectra. For the $np$ with $n>5$ states of KrD the analysis requires case (d) $p$-complexes.[9,10] For the $5p$ level, $^2\Sigma^+$ and $^2\Pi$ states have been identified and the complex fit and the two isolated states fit to the observed levels have been reported to be of similar quality, with the intensities favoring the $p$-complex description.[9] The $5p$ $^2\Pi$ state has been found to be a case (a) state in the analysis of the $4d$ $^2\Delta \rightarrow 5p$ $^2\Pi$ band.[10]

The strong coupling of these states of the rare-gas hydrides giving rise to $l$-complexes has been attributed mainly to the large dipole moment of the core cation.[12,13] Dabrowski and Sadowski have reviewed the phenomenon of $l$ uncoupling using the effective $l$-complex Hamiltonian approach,[9,10] while Jungen and Roche[13] have analyzed the $4f$ complexes of ArH and KrH using multichannel quantum defect theory and reproduced the fine structure of the observed levels.

As described above, experimental levels exist for a complete set of low-$n$ components of the $s$, $p$, $d$, and $f$ Rydberg series of KrD and they may be used along with the ionization potential of the lowest bound level to construct the entire electronic Rydberg structure of this system.[9,10] This experimental information may also be employed, along with *ab initio* calculations of the potential energy curves of the lower lying Rydberg states and those of the relevant ionic limits, to generate using quantum defect theory potential energy curves and rotational–vibrational levels for the entire manifold of Rydberg states of a particular $l\lambda$ symmetry.[14] How-

 © 2003 American Institute of Physics

Downloaded 08 Dec 2008 to 194.177.215.121. Redistribution subject to AIP license or copyright; see http://jcp.aip.org/jcp/copyright.jsp

ever, in the analyses of the observed spectra,[8–10] the nature of the lowest bound state, $A\,^2\Sigma^+$, was left as an open question, i.e., whether it is $s$ or $d$, or most likely a mixed $s+d$ state.[8,9] In the *ab initio* calculations the character of this state was obtained as Rydberg $s$ with dissociation limits of ground state Kr plus H* $(2s\,^2S)^6$. The assignment of the $l$ character of the lower states will of course determine the $l$ assignment of the higher states generated by a quantum defect calculation.

The general question of the character of the Rydberg states of rare gas hydrides, or whether they are better described as $(\mathrm{RgH}^+)e^-$ or as $(\mathrm{Rg}^+\mathrm{H})e^-$, has been addressed by Jungen *et al.*,[15] who estimate on the basis of ionization potentials and polarizabilities of the atoms involved that the most appropriate description is in terms of protonated rare gas atom with an associated electron, i.e. $(\mathrm{RgH}^+)e^-$, for the equilibrium region of the Rydberg states of all the RgH systems with Rg=He to Xe. *Ab initio* calculations on these systems,[4,6,14,16–18] have found interactions between the excited H and the excited Rg states, which are manifested as avoided crossings in the potential energy curves, especially those of the larger systems. In addition since the spherical symmetry is broken, $l$-mixing is allowed and it has been found to be important in the Rydberg spectra of ArH, KrH, and KrD.[9–13] At larger internuclear distances than the equilibrium region, e.g., at 5.0 bohr, the lowest excited states are best described by a charge transfer character, $\mathrm{Rg}^+\mathrm{H}^-$ as found, for example, in the lowest excited states of ArH and XeH,[17,18] in good agreement with existing experimental measurements of the electronic–vibrational transitions of hydrogen in solid noble gases.[19] This ion pair character is not found in the lower-lying states at the equilibrium or Rydberg region, but it will cause a series of avoided crossings in the potentials of the Rydberg states. Recent theoretical calculations on the $\mathrm{Kr}^+\mathrm{H}^-$ dimer, without taking into account the interaction with the Rydberg states, obtained for the $\mathrm{Kr}^+\mathrm{H}^-$ states minima of 5.0–5.1 eV at Kr–H distances of 2.4–2.5 Å.[20] Thus a theoretical determination of the potential energy curves of the electronic states of KrH must account for all the possible contributions to the character of the electronic states at different internuclear distances for a reasonably complete description of the electronic states of this system.

The excited states of KrH and to a smaller extent of KrD are expected to be predissociated by interaction with the repulsive ground state, by analogy with the other RgH (Rg =He, Ne, and Ar) systems. Generally stronger spectra are obtained for KrD than KrH and this difference has been attributed to differing extents of predissociation in the two systems.[8] A width of 0.5 $\mathrm{cm}^{-1}$ was reported for the observed bands involving the $A\,^2\Sigma^+$ state of KrH, whereas the corresponding lines in the deuteride were sharp.[8] Indeed almost all of the reported bands are for the Rydberg spectra of KrD.[8–10]

In the present work, a theoretical study on the Rydberg states of KrH is presented. Potential energy curves are determined with *ab initio* multireference through double excitation configuration interaction (MRDCI) calculations.[21–23] Predissociation of the lower-lying states of KrH and KrD, as well as the possible existence of a $5p$ complex made up of the $3\,^2\Sigma^+$ and $1\,^2\Pi$ states, is investigated by multistate complex scaling calculations,[14,24] where the interactions between the $X\,^2\Sigma^+$, $A\,^2\Sigma^+$, $3\,^2\Sigma^+$, and $1\,^2\Pi$ states of the *ab initio* calculations are taken into account simultaneously.

Second, the *ab initio* potentials of the lower-lying $nl$ states along with the ground state of the cation $\mathrm{KrH}^+$ (see below) are employed for a quantum defect analysis, yielding potential energy curves of higher lying $nl$ Rydberg states of KrH. In order to account for the interaction between the H*+Kr and the H+Kr* states it is necessary to use in addition an excited electronic state of the cation. The cations of rare gas hydrides, including $\mathrm{KrH}^+$, have been studied by a variety of methods. The main objective of the studies on $\mathrm{KrH}^+$ has been the determination of the ground state potentials[25–28] and there is very little published information on the excited states, either experimental or theoretical. In the recent theoretical work on the charge transfer states[20] it is stated that the calculated excited states of $\mathrm{KrH}^+$ are unbound. In the present work, in addition to the calculations on KrH, potential energy curves of the ground state $X\,^1\Sigma^+$ as well as excited singlet and triplet electronic states of $\mathrm{KrH}^+$ have been calculated in order to obtain the appropriate ionic limits for the quantum defect calculations and also in order to determine whether any bound or metastable excited electronic states of this system exist.

## II. CALCULATIONS

### A. *Ab initio* calculations

*Ab initio* MRDCI calculations have been carried out on electronic states of KrH and the cation $\mathrm{KrH}^+$, for internuclear distances between 2.0 and 10.0 bohr.

The same AO basis set was employed for the calculations on both KrH and $\mathrm{KrH}^+$. For the $K$ and $L$ shells of Kr, effective core potentials have been employed.[29] The valence AO basis set employed for Kr is that of Hurley *et al.*,[29] uncontracted and augmented with diffuse and polarization functions, $s$ (exponent 0.026), $p$ (0.0245) and $d$ (1.0,0.43,0.0212). The AO basis set for hydrogen is the $(6s/4s)$[30] augmented with two $p$ polarization functions (exponents 0.7 and 0.2) and two $s$ (0.025 and 0.007), two $p$ (0.03, 0.006) and one $d$ (0.013) diffuse functions. In this manner, $s$, $p$, and $d$ Rydberg states, correlating with excited states of both Kr and H at the dissociation limits may be calculated.

The calculations have been carried out in $C_{2V}$ symmetry, where the $^2\Sigma^+$ and the $^2\Delta$ states are obtained as $^2A_1$, and the $^2\Pi$ states as $^2B_1$, for KrH and similarily for the cation but with singlet and triplet spin multiplicity states.

The MRDCI calculations on $\mathrm{KrH}^+$ employed the molecular orbitals of the ground state $X\,^1\Sigma^+$ $(X\,^1A_1)$ as the one-electron basis and eight-electron CI calculations. Five roots of $^1A_1$ symmetry and four roots of $^1B_1$ have been calculated for $\mathrm{KrH}^+$, employing 24 and 13 reference configurations, respectively, with respect to which all single and double excitations gave rise to the configuration functions of the space of the CI calculations (121 838 for the $^1A_1$ and 81 916 for the $^1B_1$ calculations).

Nine roots of $^2A_1$ symmetry and six roots of $^2B_1$ have

Downloaded 08 Dec 2008 to 194.177.215.121. Redistribution subject to AIP license or copyright; see http://jcp.aip.org/jcp/copyright.jsp

been calculated for KrH, with MRDCI calculations employing 63 and 47 reference configurations, respectively, and a selection threshold of 0.1 $\mu$H. The molecular orbitals of the ground state $X\,^2\Sigma^+$ ($X\,^2A_1$) served as the one-electron basis and nine-electron CI calculations were carried out. The calculated energies were extrapolated to zero threshold and a full-CI correction[31] was made.

At each internuclear distance in addition to the energies, dipole transition moments between the different states and rotational–electronic coupling matrix elements between the $^2A_1$ and the $^2B_1$ states have also been calculated. Radial coupling matrix elements have also been calculated between pairs of the first three $^2A_1$ states using the finite differences method incorporated in the MRDCI programs.[32] It is expected that the radial coupling matrix elements thus calculated for states of KrH will not be as accurate as they were for HeH[33] and NeH,[14] because with increasing size of the system it becomes difficult to calculate them very precisely.[34] However, it is hoped that, as was the case in ArH,[34] the relative importance of predissociation in the three lowest excited electronic states between the hydride and the deuteride will be revealed.

### B. Quantum defect calculations

As mentioned in the Introduction, analyses of the Rydberg spectra of KrH have produced energy levels for $s$, $p$, $d$, and $f$ states as well as the ionization energy of the lowest bound state.[8–10] In the present work the calculated *ab initio* potential energy curves of the lowest $nl$ members of the $s$, $p$, and $d$ Rydberg states of KrH and the ground state of the cation are employed to generate quantum defect functions over the different values of internuclear distance, and subsequently to generate potential energy curves for the higher-lying Rydberg states. Details of the theory and the method have been presented previously.[14,35]

The potential energy curves $E(R)$ of the $l\lambda$ Rydberg states converging on the positive ion potential $V_i^+(R)$ are related to the quantum defect function $\eta_{il\lambda}(R)$, determined by

$$\tan \pi\eta_i(R) + \frac{\tan \pi\nu_i(R)}{A_{l_i}(\nu_i(R))} = 0, \tag{1}$$

where $R$ is the internuclear distance,

$$\nu_i(R) = [2(V_i^+(R) - E(R))]^{-1/2}, \tag{2}$$

and the factor $[A_{l_i}(\nu_i(R))]^{-1}$ serves to eliminate solutions with $l_i < n_i$,

$$A_{l_i}(\nu_i(R)) = \prod_{k=0}^{l_i} \left(1 - \frac{k^2}{\nu_i^2}\right). \tag{3}$$

The label $l\lambda$ is symbolic because the Born–Oppenheimer quantum defects belong to $l$-mixed states. In the present work, as was done previously in a similar calculation on NeH,[14] the states are labeled according to their predominant $l$ character.

Equation (1) is employed first, with the *ab initio* potentials for the lowest $n\ l\lambda$ states substituted for $E(R)$, for the determination of the quantum defect functions. The higher Rydberg states are calculated subsequently, again using Eq. 1, but this time by introducing the calculated quantum defect functions and varying $E(R)$, at each $R$ specified to find those energies which satisfy the equation.

In general, there is some energy dependence in the quantum defects calculated as above and this may be incorporated by using in addition the potential energy curves of the second lowest $n\ l\lambda$ states, in the $\eta_{il\lambda}(R)$ functions and the subsequent calculation of higher Rydberg states.

Further details of the quantum defect calculations of the present work shall be presented along with their results.

### C. Complex scaling calculations

The *ab initio* potential energy curves of the $X\,^2\Sigma^+$, $A\,^2\Sigma^+$, $3\,^2\Sigma^+$, and $1\,^2\Pi$ states and their interaction matrix elements, radial coupling for $^2\Sigma^+$-$^2\Sigma^+$ and rotational–electronic coupling for $^2\Sigma^+$-$^2\Pi$, calculated at different $R$, are employed for a four-state complex coordinate calculation. Vibrational levels of the interacting states and their predissociation widths are calculated, in both KrH and KrD, for different rotational levels, taking values from $J=1$ to $J=50$. The method employed involves the diagonilization of a complex Hamiltonian matrix where all the possible interactions have been included. Details of the method can be found elsewhere,[14,24,36] with only a brief outline given here.

The transformation of the nuclear coordinate $R \rightarrow \rho = \mathrm{R}e^{i\theta}$ with $\theta$ real, allows the calculation of energies and widths of predissociation resonances in terms of square integrable functions. A complex eigenvalue problem is solved,

$$|\underline{\underline{H}} - \underline{\underline{z}}| = 0, \tag{4}$$

where $\underline{\underline{z}}$ is the diagonal matrix of complex eigenvalues. The resonances correspond to the eigenvalues $z_k$ which are stable with respect to variations in $\theta$ and

$$z_k = E_k - \frac{i}{2}\Gamma_k \tag{5}$$

with $E_k$ the energy position and $\Gamma_k$ the linewidth of the resonance. The predissociation lifetime $\tau$ in seconds is obtained from the linewidth $\Gamma$ in atomic units using

$$\tau = \frac{2.418\,88 \times 10^{-17}}{\Gamma}. \tag{6}$$

The Hamiltonian matrix in Eq. (4) consists of blocks $\underline{\underline{H}}^{IJ}$ where $I,J$ stand for the different electronic states. A basis set of harmonic oscillator functions is employed, and the required integrals are evaluated analytically for the kinetic energy and numerically for the potential energy operator.[14,24,36]

Equation (4) is set up and solved for a given basis set size at different values of $\theta$ and the stable eigenvalues $z_k$ with respect to $\theta$ correspond to the required resonances. Convergence with respect to the basis set size is also sought. After exploratory convergence calculations with different numbers of basis functions, a basis set of 120 Hermite polynomials for each electronic state has been employed for the present calculations on KrH and KrD. The eigenvalues are stable for $\theta$ values up to 10. These results will be presented in subsequent sections.

Downloaded 08 Dec 2008 to 194.177.215.121. Redistribution subject to AIP license or copyright; see http://jcp.aip.org/jcp/copyright.jsp

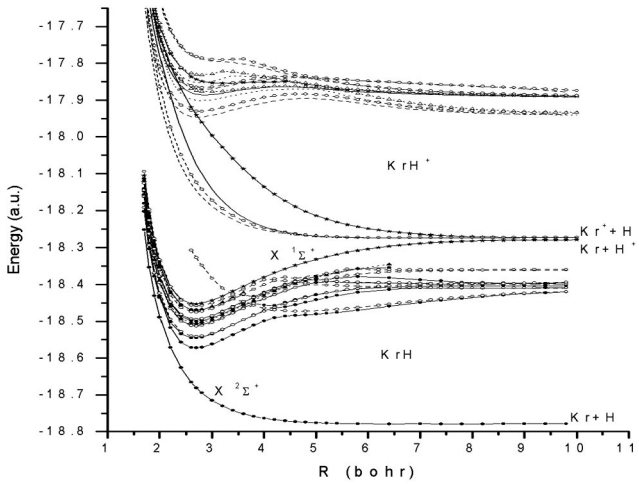


FIG. 1. *Ab initio* potential energy curves for electronic states of KrH and $KrH^+$. Solid solid circles stand for $^2\Sigma^+$ states, open circles for $^2\Pi$, and solid triangles for $^2\Delta$.

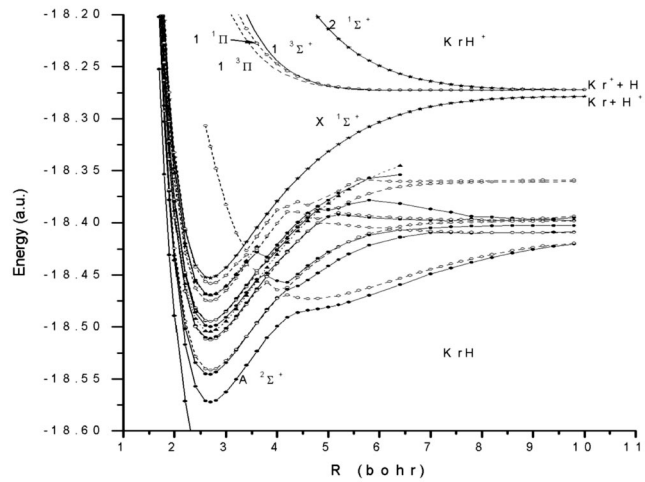


FIG. 2. *Ab initio* potential energy curves for excited electronic states of KrH.

## III. RESULTS AND DISCUSSION

### A. Potential energy curves

An overview of the potential energy curves of the electronic states of KrH and $KrH^+$ calculated in the present work is given in Fig. 1. As shown therein, the ground state of KrH is repulsive. The present calculations obtain for the ground state potential a minimum of 137 $cm^{-1}$ at 6.4 bohr compared to the experimental value for the well depth of 48 $cm^{-1}$ at $R_m$ of 6.75 bohr. The excited states of KrH have Rydberg minima at an internuclear distance of 2.7 bohr and their potential energy curves closely resemble that of the ground state of $KrH^+$. At larger internuclear distances the potential energy curves of the excited states of KrH have avoided crossings resulting from interactions of states with different character, including interactions with the ion pair $Kr^+H^-$ states, which are the lowest excited $^2\Sigma^+$ and $^2\Pi$ states of KrH at $R$ larger than 4.5 bohr.

The singlet and triplet electronic states of the cation $KrH^+$ are also plotted in Fig. 1. As shown, the ground state is the only state of $KrH^+$ with a substantial minimum. The calculated potential energy curve for the ground state $X\,^1\Sigma^+$ has $r_e$ of 2.668 bohr (1.412 Å), $D_e$ of 4.74 eV and $\omega_e$ of 2508 $cm^{-1}$, $\omega_e x_e$ of 43 $cm^{-1}$, obtained from a fit to vibrational levels calculated with this potential. These values are close to experimental ($D_e = 4.81$ eV, $r_e = 1.4212$ Å, $\omega_e = 2494$ $cm^{-1}$, $\omega_e x_e = 48.53$ $cm^{-1}$)[25,26] and other theoretical values ($D_e = 4.81$ eV, $r_e = 1.419$ Å, $\omega_e = 2561$ $cm^{-1}$, $\omega_e x_e = 49$ $cm^{-1}$).[27]

The dissociation limit of the ground state of $KrH^+$ is $Kr(4p^6\,^1S) + H^+$. The next higher dissociation limit, $Kr^+$ $(4p^5\,^2P) + H$ (is $^2S$), is very close to the first limit, lying at 3292 $cm^{-1}$ above it. With this limit correlate states $^1\Sigma^+$, $^3\Sigma^+$, $^1\Pi$, and $^3\Pi$, which are all repulsive (see Fig. 1). The lowest of these states is the second ionic limit, which is reflected in the character and the potential energy curves of some of the Rydberg states of KrH at large $R$ (e.g., the second and fourth $^2\Pi$ states of KrH at $R$ larger than 4.5 bohr). The next higher excited states, above the four repulsive states correlate with dissociation limits $Kr^+ + H^*$ and $Kr^* + H^+$. Their potential energy curves resemble those of the Rydberg states of the neutral molecule (see Fig. 1), with minima at the $KrH^+$ ground state equilibrium bond length. However, in this case the minima are only local minima and the states are metastable. The deepest wells are calculated for the $2\,^1\Pi$ and $2\,^3\Pi$ states, with depths of 1.27 eV at 2.8 bohr and 1.38 eV at 2.7 bohr, respectively, with respect to the barriers found in their potential energy curves at 4.8 bohr.

A close-up of the potentials of the excited states of KrH is given in Fig. 2, where the ionic limits are also plotted. As shown in Fig. 2, the excited states all have similar minima at $R$ of 2.7 bohr. At larger $R$, there are avoided crossings with states of different character (see Fig. 2). As mentioned above, the two lowest excited states at internuclear distance larger than 4.5 bohr are the $Kr^+H^-$ $^2\Sigma^+$ and $^2\Pi$ states. The $^2\Pi$ charge transfer state, is clearly indicated. It has a wide minimum at 4.6–4.8 bohr and rises sharply at shorter distances, crossing the stack of $^2\Pi$ Rydberg states (avoided crossings in the adiabatic description). The corresponding $^2\Sigma^+$ state, is not manifested as clearly, with no obvious minimum in the adiabatic state (cf. Fig. 2) but rather a shoulder between 4.5 and 6.0 bohr. It may be roughly followed in the set of avoided crossings of the higher Rydberg $^2\Sigma$ states, running parallel to $^2\Pi$ $Kr^+H^-$. However, within the nine $^1A_1$ roots calculated it was not possible to follow this state (as was possible for the $^2\Pi$ $Kr^+H^-$) at short bond lengths and at energies higher than the ground state potential of $KrH^+$ (see Fig. 2). The vertical transition energy from the ground state at 4.7 bohr is 7.90 eV and 8.20 eV for the $^2\Sigma^+$ and the $^2\Pi$ $Kr^+H^-$ states, respectively. There are no experimental data for the diatomic $Kr^+H^-$ exciplex and the observed emission of hydrogen-doped solid krypton matrices has been attributed to $(Kr_6H)^*$ and $(Kr_2^+H^-)^*$.[19] The present results are in agreement with previous theoretical calculations on $Kr^+H^-$, yielding vertical transition energies from the ground state of 7.91, 7.97, and 8.54 eV with $R_0$ of 4.72, 4.54, and 4.54 bohr for the states correlating with the limits $Kr^+$ 3/2, 3/2, and 1/2, respectively.[20]

Downloaded 08 Dec 2008 to 194.177.215.121. Redistribution subject to AIP license or copyright; see http://jcp.aip.org/jcp/copyright.jsp

TABLE I. Observed levels in KrD (Ref. 9) and *ab initio* vertical transition energies and radiative transition probabilities at Kr–H distance of 2.7 bohr, for transitions from higher excited states to the $A\,^2\Sigma^+$ state in KrH.

| | Present work (*ab initio*) | | | Present work |
|---|---|---|---|---|
| Observed levels (Ref. 9) | Upper state | $\Delta E$ ($cm^{-1}$) | Jungen *et al.* (Ref. 15) | Trans. prob. ($s^{-1}$) |
| 25 030 $9p$ | $5\,^2\Pi\ p$ | 25 149 | | $0.159E+08$ |
| 24 266 $7d\,^2\Pi$ | | | | |
| 23 920 $8p$[b] | | | | |
| 23 324 $5f$ | | | | |
| 22 614 $6d\,^2\Pi$ | | | | |
| 21 950 $7p$[b] | | | | $0.405E+07$ |
| | $2\,^2\Delta\ d$ | 22 762 | | |
| 21 413 $6d\,^2\Sigma^+$ | $7\,^2\Sigma^+\ (s+p+d)$[c] | 22 768 | | |
| 20 845 $4f$ | | | 207 18–207 62[d] | |
| 20 370 $7s\,^2\Sigma^+$ | | | | |
| 19 425 $5d\,^2\Pi$ | $4\,^2\Pi\ d$ | 21 421 | | $0.289E+06$ |
| 17 840 $6p$[b] | $6\,^2\Sigma^+\ (s+p)$ | 17 165 | | $0.396E+07$ |
| 17 840 $6p$[b] | $3\,^2\Pi\ (p+d)$ | 17 055 | | $0.285E+05$ |
| 16 580 $5d\,^2\Sigma^+$ | $5\,^2\Sigma^+\ (s+p+d)$[c] | 15 950 | | $0.669E+05$ |
| 14 250 $4d\,^2\Delta$ | $1\,^2\Delta\ d$ | 14 850 | 144 97 | |
| 14 205 $6s\,^2\Sigma^+$ | $4\,^2\Sigma^+\ (d+s+p)$[c] | 13 404 | 147 68 | $0.658E+04$ |
| 12 280 $4d\,^2\Pi$ | $2\,^2\Pi\ (d+p)$ | 13 141 | 11 494 | $0.364E+07$ |
| 7216 $5p\,^2\Pi$ | $1\,^2\Pi\ (p+d)$ | 6793 | 8024 | $0.801E+07$ |
| 6480 $5p\,^2\Sigma^+$ | $3\,^2\Sigma^+\ p+s$ | 5853 | 5461 | $0.279E+07$ |
| 0 $5s$, $4d\,^2\Sigma^+$ | $A\,^2\Sigma^+\ s$ | 0[a] | 1358 | |

[a]Calculated total energy for the $A\,^2\Sigma^+$ state at 2.7 bohr is $-18.572\,228$ hartree and for the ground state $X\,^2\Sigma -18.681\,158$ hartree.
[b]$E_\Pi - E_\Sigma$ : 9.5, 28.7, and 102.4 $cm^{-1}$ for the $8p$, $7p$, and $6p$ complexes, respectively (Ref. 9).
[c]$s \leftrightarrow d$ reassignment of experimental levels.
[d]Reference 13.

As shown in Fig. 2, in the present work, six $^2\Sigma^+$, five $^2\Pi$ and two $^2\Delta$ Rydberg states of KrH have been obtained in the *ab initio* calculations. In Table I, the observed levels in KrD[9] are given along with the transition energies and radiative lifetimes for bound–bound transitions to the lowest excited electronic state of KrH, $A\,^2\Sigma^+$, of the present *ab initio* calculations and transition energies calculated by Jungen *et al.*[15] The observed $nf$ levels have been included in Table I for completeness, $f$-type Rydberg states have not been calculated in the present work. The $l$-character of the *ab initio* states calculated in the present work is also indicated in the second column of Table I, where for mixed-$l$ states the predominant character is given first. As shown, the theoretical transition energies of the present work are very close to the theoretical values of Jungen *et al.*[15] They are also in reasonable agreement with the experimental values and with most recent assignment of the $np\ ^2\Sigma^+$ and $^2\Pi$ levels and the $nd$ $^2\Pi$ and $^2\Delta$ levels.[9] However, according to the present calculations the $A\,^2\Sigma^+$ state has $s$ character, $4\,^2\Sigma^+$ has predominantly $d$ character and $5\,^2\Sigma^+$ has $s$ character, while Dabrowski *et al.*[8–10] consider $A\,^2\Sigma^+$ as either $5s$ or $4d$ and they would favor it to have a $4d$-mixed-with-$s$ character. In addition, they assign as $6s$ and $5d$ the levels corresponding to the fourth $^2\Sigma^+$ and fifth $^2\Sigma^+$ states, respectively (see Table I). The present *ab initio* results obtain the three $4d$ states ($2\,^2\Pi$, $4\,^2\Sigma^+$ and $1\,^2\Delta$) in sequence and below the $6s$ $5\,^2\Sigma^+$ state.

As shown in Table I, some of the observed $ns$, $np$, and $nd$ levels are missing (e.g., $7p\,^2\Pi$ and $8p\,^2\Sigma^+$, $^2\Pi$ states in the $np$ manifold) in the *ab initio* calculations. In general, it is difficult to calculate by *ab initio* methods the higher-lying roots of a given symmetry, and a large number of diffuse functions are required for the Rydberg states, which may lead to linear dependencies, if diffuse functions are used on both centers. A more natural calculation of the higher-lying Rydberg states is possible with a quantum defect method, based on the potentials of the lower members of each $nl$ series and the potential of the relevant ionic limit. The results of quantum defect calculations on the Rydberg states of KrH are described in the next section.

### B. Results of the quantum defect calculations

The *ab initio* energies of the lowest $nl\lambda$ states at different $R$ have been employed for the calculation of quantum defects as described previously in Sec. II B. For the quantum defects of the $ns$ Rydberg states, the *ab initio* potential of the $A\,^2\Sigma^+$ state was employed as $5s$ and it was shifted by $-0.006\,812$ hartree in order to fit the experimental ionization energy of 27 727 $cm^{-1}$. The *ab initio* potential of the $3\,^2\Sigma^+$ and $1\,^2\Pi$ $5p$ states, shifted by $-0.004\,076$ and $-0.004\,726$ hartree, respectively, were employed for the quantum defects of the $np\ ^2\Sigma^+$ and $^2\Pi$ states. Similarily the potential of $4d$ $2\,^2\Pi$, shifted by $-0.010\,404$ hartree, of $4d$ $4\,^2\Sigma^+$ shifted by $-0.003\,249$ hartree, and of $4d$ $1\,^2\Delta$, shifted by $-0.009\,646$ hartree, were employed for calculation of quantum defect functions of the $nd\ ^2\Pi$, $^2\Sigma^+$, and $^2\Delta$ states, respectively. These shifts were necessary in order to place the Rydberg states in the correct energy with respect to the ionic state, at 2.7 bohr. As mentioned previously, the $l$-character was assigned on the basis of its predominance in the character of the *ab initio* calculated states at the minimum (see Table I). The adiabatic *ab initio* potentials for $R$ only up to 4.0 bohr have been employed, because for larger $R$ the character of the Rydberg states changes and there are many avoided

Downloaded 08 Dec 2008 to 194.177.215.121. Redistribution subject to AIP license or copyright; see http://jcp.aip.org/jcp/copyright.jsp

TABLE II. Expansion coefficients of the quantum defect functions [cf. Eq. (7)].

| Coefficient channel | $a_0$ | $a_1$ | $a_2$ | $a_3$ | $a_4$ |
|---|---|---|---|---|---|
| $^2\Sigma^+$ 5$s$ | 8.602 13 | −9.931 98 | 6.049 68 | −1.545 03 | 0.141 843 |
| $^2\Sigma^+$ 6$s$ | 14.424 7 | −18.8000 | 10.9760 | −2.762 79 | 0.255 281 |
| $^2\Sigma^+$ 5$p$ | −11.213 3 | 15.4004 | −7.985 34 | 1.806 04 | −0.150 709 |
| $^2\Sigma^+$ 6$p$ | −5.409 06 | 5.771 96 | −2.251 67 | 0.331 433 | −0.011 767 |
| $^2\Pi$ 5$p$ | 0.283 308 | −0.937 593 | 0.484 541 | −0.105 776 | 0.008 565 |
| $^2\Pi$ 6$p$ | −14.6186 | 23.9464 | −14.8475 | 4.009 89 | −0.396 864 |
| $^2\Sigma^+$ 4$d$ | 2.159 118 | −2.841 197 | 1.545 126 | −0.363 531 | 0.031 520 |
| $^2\Delta$ 4$d$ | 2.024 11 | −2.682 12 | 1.456 03 | −0.336 827 | 0.028 1438 |
| $^2\Pi$ 4$d$ | 0.071 9865 | −1.107 86 | 0.644 331 | −0.155 330 | 0.013 384 |

crossings in the calculated potentials. In addition the charge-transfer states have not been included in the quantum defect analysis.

The quantum defects obtained at different values of $R$, from 1.8 to 4.0 bohr, are expressed in terms of a polynomial of fourth order.

$$\eta_i(R)=\sum_{j=0}^{4} a_j R^j. \tag{7}$$

The resulting expansion coefficients are given in Table II. For the *ns* and *np* states, the coefficients for the quantum defects obtained from the two lowest $nl\lambda$ states are given, illustrating the energy dependence of the calculated quantum defect functions corresponding to the *ab initio* curves. For the $nd$ $^2\Sigma^+$, $^2\Pi$, and $^2\Delta$ states only the $4d\lambda$ states were employed. This is because the $5d\lambda$ states are among the highest *ab initio* roots and they were not considered as reliable as the lower roots. The above expansions for the quantum defect functions for the $5s$, $5p$, and $4d$ Rydberg states have been employed for the calculation of the electronic energies $E(R)$ for higher $n$ Rydberg states, for $R$ up to 4.0 bohr.

In Table III vertical transition energies at 2.7 bohr are listed for transitions from higher $nl\lambda$ states to $5s$ $^2\Sigma^+$, calculated from the potentials generated by the above quantum defect calculations, along with experimental values.[9] Two theoretical values of the transition energies are given in Table III for the *ns* and the *np* states. The first one was obtained using the quantum defects of the lowest $nl\lambda$ state while for the second value the quantum defects of the second $nl\lambda$ state were also used. As shown in Table III, the energy dependence of the quantum defects leads to very similar transition energies for the *np* states, with differences between the two theoretical values of only 50–250 cm$^{-1}$. For the *ns* states the energy dependence has a bigger effect on the calculated levels, especially for the $7s$ and $6s$ levels, with differences in the calculated transition energies of 623 cm$^{-1}$ and 1141 cm$^{-1}$, respectively. These results show that the adiabatic potential energy curve of the $A$ $^2\Sigma^+$ state is not as representative for the higher *ns* states as the $5p$ $3$ $^2\Sigma^+$ state is for the $np$ $^2\Sigma^+$, but the general picture is not altered. There is excellent agreement of the transition energies obtained from the quantum-defect generated potentials with experimental quantities. The $np$ $^2\Sigma^+$ and $^2\Pi$ states are calculated very close to each other, with the calculated $E_\Pi - E_\Sigma$ of 16 cm$^{-1}$, for $n=9$, and 30, 60, and 160 cm$^{-1}$ for $n=8$, 7,

TABLE III. Transition energies from $5s$ $A$ $^2\Sigma^+$ at 2.7 bohr obtained from the potentials generated by the quantum defect calculations. Upper value only the potential of lowest energy $nl$ state used (indicated by *), lower value the potentials of the second lowest state also used (indicated by **), see text. Experimental values (Ref. 9) are given in parentheses, which have been reassigned, $s \leftrightarrow d$, in the present work.

| $ns$ | $s$ $^2\Sigma^+$ | $np$[a] | $p$ $^2\Sigma^+$ | $p$ $^2\Pi$ | $nd$ | $d$ $^2\Sigma^+$ | $d$ $^2\Pi$ | $d$ $^2\Delta$ |
|---|---|---|---|---|---|---|---|---|
| 10 | 25 609 | 9 | 25 096 | 25 128 | 8 | 25 448 | 25 321 | 25 454 |
| | 25 751 | | 25 146 | 25 162 | | | 25 398 | |
| | | | (25 030) | (25 030) | | | | |
| 9 | 24 795 | 8 | 23 953 | 24 007 | 7 | 24 544 | 24 335 | 24 554 |
| | 25 011 | | 24 032 | 24 062 | | | 24 443 | |
| | | | (23 920) | (23 920) | | | (24 266) | |
| 8 | 23 442 | 7 | 21 918 | 22 020 | 6 | 23 028 | 22 644 | 23 046 |
| | 23 796 | | 22 051 | 22 111 | | | 22 823 | |
| | | | (21 950) | (21 950) | | | (22 614) | |
| 7 | 20 947 | 6** | 17 730 | 17 962 | 5 | 20 224 | 19 412 | 20 257 |
| | 21 570 | | 17 951 | 18 111 | | | 19 704 | |
| | (21 413)[b] | | (17 840) | (17 840) | | (20 370)[c] | (19 425) | |
| 6** | 15 540 | 5* | 6620 | 7361 | 4* | 14 348 | 12 429 | 14 409 |
| | 16 681 | | 6620 | 7361 | | | 12 432 | (14 250) |
| | (16 580)[b] | | (6480) | (7216) | | (14 205)[c] | (12 280) | |
| 5* | 0 | | | | | | | |

[a] $E_\Pi - E_\Sigma$ : 9.5, 28.7, and 102.4 cm$^{-1}$ for the $8p$, $7p$, and $6p$ complexes, respectively (Ref. 9).

Downloaded 08 Dec 2008 to 194.177.215.121. Redistribution subject to AIP license or copyright; see http://jcp.aip.org/jcp/copyright.jsp

TABLE IV. Transition energies ($cm^{-1}$) obtained from the quantum defect energies for some bound–bound transitions in KrH, with $5p\ 3\,^2\Sigma^+$ and $5p\ 1\,^2\Pi$ as lower states. Experimental values in parentheses.

| Upper state | $\Delta E(\rightarrow 3\,^2\Sigma^+\ 5p)$ | $\Delta E(\rightarrow 1\,^2\Pi\ 5p)$ |
|---|---|---|
| $3\,^2\Delta\ (6d)$ | 16 425 | 15 685 |
| $10^2\Sigma^+\ (6d)$ | 16 407 | 15 667 |
| $6\,^2\Pi\ (6d)$ | 16 202 (16 138[b]) | 15 462 |
| $5\,^2\Pi\ (7p)$ | 15 490 | 14 750 |
| $9\,^2\Sigma^+\ (7p)$ | 15 430 | 14 690 |
| $8\,^2\Sigma^+\ (7s)$ | 14 949 (14 934[b]*) | 14 209 |
| $2\,^2\Delta\ (5d)$ | 13 636 | 12 896 |
| $7\,^2\Sigma^+\ (5d)$ | 13 603 (13 890[b]*) | 12 863 |
| $4\,^2\Pi\ (5d)$ | 13 083 (12 944[b]) | 12 343 |
| $3\,^2\Pi\ (6p)$ | 11 490 | 10 750 |
| $6\,^2\Sigma^+\ (6p)$ | 11 330 | 10 591 |
| $5\,^2\Sigma^+\ (6s)$ | 10 060 (10 146[b]*) | 9320 |
| $1\,^2\Delta\ (4d)$ | 7788 | 7047 (7100[c]) |
| $4\,^2\Sigma^+\ (4d)$ | 7727 (7725[b]*) | 6987 |
| $2\,^2\Pi\ (4d)$ | 5811 (5815[b]) | 5071 |
| $1\,^2\Pi\ (5p)$ | 740 (735[a]) | 0 |
| $3\,^2\Sigma^+\ (5p)$ | 0 | |

[a]Reference 10.
[b]Reference 9, assignments of Ref. 10.
[b*]Reference 10, different assignments.

and 6, respectively (using the values obtained from the quantum defect functions with the energy dependence), with corresponding experimental values of 9.5, 28.7, and 102.4 $cm^{-1}$ for $n=8$, 7, and 6, respectively,[9] consistent with the treatment of these states as *np* complexes in the analyses of the Rydberg spectra.[9,10] The $5p\ ^2\Sigma^+$ and $^2\Pi$ states are further apart, by 735 $cm^{-1}$, and accordingly they have been treated both separately and as forming a *p* complex in the analyses of the Rydberg spectra of KrD.[8,9]

Again, the two $nd\ ^2\Sigma^+$ levels of Dabrowski and Sadovski,[9] $5d$ at 16 580 $cm^{-1}$ and $6d$ at 21 413 $cm^{-1}$, are in better agreement with levels $6s$ and $7s$, even without the energy dependence (see Table III) and conversely their $6s$ and $7s$ levels at 14 205 $cm^{-1}$ and 20 370 $cm^{-1}$, correspond better to the theoretical $4d$ and $5d\ ^2\Sigma^+$ levels, respectively (see Table III). The present results are a direct consequence of the fact that the $A\,^2\Sigma^+$ state is found in the *ab initio* calculations to have *s* character rather than $4d$, and the $4\,^2\Sigma^+$ state is found to have predominantly *d* character and is used as the $4d$ state in the quantum defect calculations.

In Table IV, some further comparisons are made with available experimental transition energies,[8] for transitions from higher Rydberg states to $5p\ 3\,^2\Sigma^+$ and $1\,^2\Pi$. The experimental assignments are according to the modifications proposed subsequently, reassigning the *np* upper states to $nd$.[9] As shown there is excellent agreement between theoretical transition energies and the experimental for transitions to $5p\ 3\,^2\Sigma^+$. There is only one experimental band reported for transitions with $5p\ ^2\Pi$ as lower state, at 7100 $cm^{-1}$, assigned to $4d\ ^{2\Delta}\rightarrow 5p\ ^2\Pi$,[10] for which the theoretical value is in excellent agreement, at 7047 $cm^{-1}$. Thus except for the "switching" required for the assignments of the $nd$ ($n=4,5$) and $ns$ ($n=6,7$) states, in Table III, the present theoretical transition energies are in excellent agreement with the experimental values.

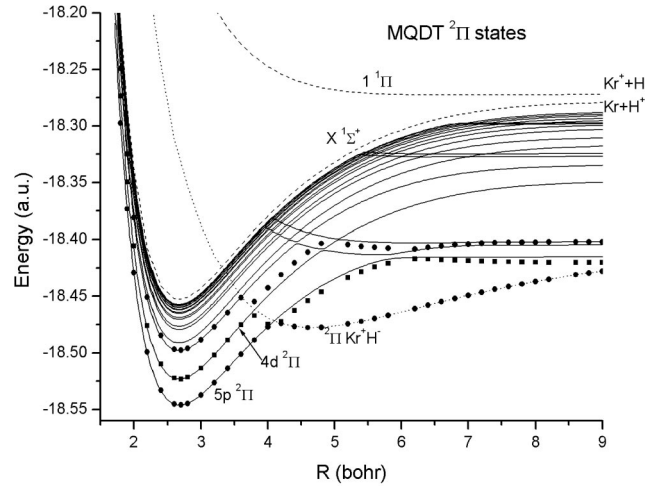


FIG. 3. Potential energy curves for states of KrH generated by the four-channel quantum defect calculations. Solid circles stand for *ab initio* points.

In the quantum defect calculations described thus far, only Rydberg states converging to the first ionic limit have been considered. Therefore the generated potentials give the adiabatic potentials only near the potential well, for $R$ less than about 4.0 bohr. In order to generate the full adiabatic potential energy curves it is necessary to consider the second ionic limit, to which the Kr*–H states converge. Such a calculation has been carried out in the present work for the $^2\Pi$ states of KrH, involving four channels consisting of $5p$ and the $4d\ ^2\Pi$ Rydberg states and two Kr*–H states, as obtained in the *ab initio* calculations for $R$ greater than 4.0 bohr. Two ionic limits are employed, the ground state $X\,^1\Sigma^+$ and the $1\,^1\Pi$ of $KrH^+$. The lack of *ab initio* data at short $R$ for the two repulsive Kr*–H states makes it necessary to use a constant quantum defect for each of these states, i.e., making the assumption that they rise up parallel to their ionic limit. A small constant interaction of 0.02 hartree between the various channels is introduced, as required for the avoided crossings. For a multichannel treatment a generalization of Eq. (1) is used.[35] The resulting potentials for the $^2\Pi$ states have been plotted in Fig. 3, showing the $5p$ and $4d\ ^2\Pi$ Rydberg states, with the avoided crossings with the Kr*–H states propagated up to higher $n$ levels. The *ab initio* points of the lowest three $^2\Pi$ states have also been plotted for comparison while a diabatic potential energy curve for the charge transfer state, constructed by following through the crossings with the Rydberg states in the adiabatic potentials, is also included in Fig. 3, for completeness. Thus it is possible to reproduce the adiabatic *ab initio* potential energy curves, and to propagate them to higher $n$ levels, provided that sufficient experimental levels are known as well as the potential energy curves of the relevant ionic limits.

### C. Results of the complex coordinate calculations

The *ab initio* data employed for these calculations have been plotted in Fig. 4, where the potential energy curves of the four states, the radial coupling matrix elements between pairs of the $^2\Sigma^+$ states and the rotational–electronic coupling matrix elements between the $1\,^2\Pi$ and each of the $^2\Sigma^+$

Downloaded 08 Dec 2008 to 194.177.215.121. Redistribution subject to AIP license or copyright; see http://jcp.aip.org/jcp/copyright.jsp

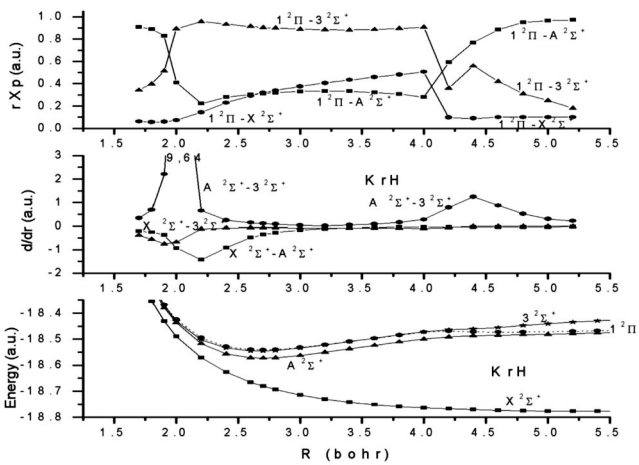


FIG. 4. *Ab initio* potentials and coupling matrix elements employed in the four-state complex coordinate calculations.

states. As shown, the biggest radial coupling interaction is obtained between the two excited $^2\Sigma^+$ states, and similarly the biggest rotational–electronic coupling is calculated between the $5p$ $1\,^2\Pi$ and $3\,^2\Sigma^+$ states. Predissociation can occur by interactions with the repulsive ground state. As shown in Fig. 4, the $X\,^2\Sigma^+ - A\,^2\Sigma^+$ radial coupling is larger than the $X\,^2\Sigma^+ - 3\,^2\Sigma^+$ in the region of the potential energy wells, while the rotational electronic coupling $X\,^2\Sigma^+ - 1\,^2\Pi$ is small in the region of interest (cf. Fig. 4).

The results of the multi-state vibrational calculations on the $X\,^2\Sigma^+$, $A\,^2\Sigma^+$, $1\,^2\Pi$, and $C\,^2\Sigma^+$ states are summarized in Tables V and VI for KrH and KrD, respectively. Vibrational levels are given for rotational level $N=10$, in $\mathrm{cm}^{-1}$ with respect to the level $v=0$, $N=1$, along with the squares of coefficients of the above three excited states, the half-widths in atomic units and the corresponding predissociation lifetimes in seconds. Results for different values of $N$, ranging from 1 to 20, can be obtained directly from the authors.

As shown in Tables V and VI, there is some mixing of the levels of the $A\,^2\Sigma^+$ and $C\,^2\Sigma^+$ states and there is also interaction with the levels of the $B\,^2\Pi$ state for high rotational levels (cf. results for $N=10$). Similar results as for $N=10$ have been obtained for $N=20$.

The present results do not show the formation of a $5p$ $(\Sigma^+,\Pi)$ complex in KrH and in KrD as a result of the rotational–electronic coupling, since even for $N=20$ the $B\,^2\Pi$ state does not mix very heavily with the $A\,^2\Sigma^+$ and $C\,^2\Sigma^+$ states. As mentioned in the Introduction, while the existence of the $n>5$ $np$ complexes in KrD is necessary for the explanation of the observed rotational structure the $5p$ states can be considered as isolated states with equal quality in the fit as for a $5p$ complex. It may be of interest to treat by similar CCR calculations the interactions between the higher members of the series of $np$ complexes in KrD.

As shown in Table V, predissociation is significant in KrH, especially for the levels of the $A\,^2\Sigma^+$ state, and it increases for higher vibrational levels. The calculated half-width for the $v=0$ level of this state is $0.3622\times10^{-5}$ hartree, or a width ($\Gamma$) of $1.59\ \mathrm{cm}^{-1}$. This value is about three times larger than the reported experimental width of $0.5\ \mathrm{cm}^{-1}$. Predissociation is also important for the levels of the $C\,^2\Sigma^+$ in KrH, but is not significant for the levels of the $B\,^2\Pi$ state for $N=1$ while with increasing $N$ (cf. for $N=10$ in Table V) it gains some importance. In KrD, predissociation is not very significant for low vibrational levels, as shown in Table VI, even for the $^2\Sigma^+$ states. The calculated width for the $v=0$ level of $A\,^2\Sigma^+$ in KrD is smaller than the corresponding width in KrH by a factor of 60. This is in agreement with the experimental observations that the states of KrH are more predissociated than those of KrD.[8]

## IV. CONCLUSION

In the present work a theoretical study of the Rydberg states of KrH is presented and where possible the results are compared to experimental observations. *Ab initio* and quantum defect calculations have been employed and potential energy curves have been determined for $nl\lambda$ Rydberg states of KrH. The transition energies obtained from the quantum defect calculations, calculated at an internuclear distance of

TABLE V. Energies, mixing coefficients, half-widths and predissociation lifetimes of vibrational levels of the $A\,^2\Sigma^+$, $3\,^2\Sigma^+$, and $1\,^2\Pi$ states of KrH, for rotational level $N=10$.

| | $E^a$ ($\mathrm{cm}^{-1}$) | $c^2(A\,^2\Sigma^+)$ | $c^2(3\,^2\Sigma^+)$ | $c^2(1\,^2\Pi)$ | $\Gamma/2$ (hartree) | Lifetime(s) |
|---|---|---|---|---|---|---|
| $A\,^2\Sigma^+$ $v=0$ | 885 | 0.9993 | 0.0002 | 0.0000 | 0.3235*E*-05 | 0.38*E*-11 |
| $A\,^2\Sigma^+$ $v=1$ | 3415 | 0.9978 | 0.0007 | 0.0000 | 0.1114*E*-04 | 0.11*E*-11 |
| $A\,^2\Sigma^+$ $v=2$ | 5831 | 0.9959 | 0.0016 | 0.0000 | 0.2261*E*-04 | 0.53*E*-12 |
| $3\,^2\Sigma^+$ $v=0$ | 7287 | 0.0009 | 0.9776 | 0.0215 | 0.5414*E*-06 | 0.22*E*-10 |
| $1\,^2\Pi$ $v=0$ | 8031 | 0.0000 | 0.0214 | 0.9785 | 0.8098*E*-08 | 0.15*E*-08 |
| $A\,^2\Sigma^+$ $v=3$ | 8131 | 0.9947 | 0.0015 | 0.0000 | 0.3649*E*-04 | 0.33*E*-12 |
| $3\,^2\Sigma^+$ $v=1$ | 9770 | 0.0007 | 0.9737 | 0.0256 | 0.4894*E*-06 | 0.25*E*-10 |
| $A\,^2\Sigma^+$ $v=4$ | 10 307 | 0.9914 | 0.0032 | 0.0003 | 0.5367*E*-04 | 0.23*E*-12 |
| $1\,^2\Pi$ $v=1$ | 10 428 | 0.0003 | 0.0256 | 0.9742 | 0.5005*E*-09 | 0.24*E*-07 |
| $3\,^2\Sigma^+$ $v=2$ | 12 112 | 0.0557 | 0.9171 | 0.0270 | 0.8003*E*-03 | 0.15*E*-11 |
| $A\,^2\Sigma^+$ $v=5$ | 12 358 | 0.9314 | 0.0588 | 0.0040 | 0.7165*E*-04 | 0.17*E*-12 |
| $1\,^2\Pi$ $v=2$ | 12 710 | 0.0008 | 0.0301 | 0.9691 | 0.4471*E*-10 | 0.27*E*-06 |
| $A\,^2\Sigma^+$ $v=6$ | 14 101 | 0.6116 | 0.3790 | 0.0054 | 0.9929*E*-04 | 0.12*E*-12 |
| $3\,^2\Sigma^+$ $v=3$ | 14 472 | 0.3849 | 0.5799 | 0.0327 | 0.1358*E*-04 | 0.89*E*-12 |
| $1\,^2\Pi$ $v=3$ | 14 885 | 0.0049 | 0.0333 | 0.9618 | 0.1357*E*-06 | 0.89*E*-10 |

[a]Energy given with respect $-18.572\,920$ hartree.

Downloaded 08 Dec 2008 to 194.177.215.121. Redistribution subject to AIP license or copyright; see http://jcp.aip.org/jcp/copyright.jsp

TABLE VI. Energies, mixing coefficients, half-widths and predissociation lifetimes of vibrational levels of the $A\,^2\Sigma^+$, $3\,^2\Sigma^+$, and $1\,^2\Pi$ states of KrD for rotational level $N=10$.

| | $E^a$ (cm$^{-1}$) | $c\,^2(A\,^2\Sigma^+)$ | $c\,^2(3\,^2\Sigma^+)$ | $c\,^2(1\,^2\Pi)$ | $\Gamma/2$ (hartree) | Lifetime(s) |
|---|---|---|---|---|---|---|
| $A\,^2\Sigma^+$ $v=0$ | 451 | 0.9998 | 0.0001 | 0.0000 | 0.52454$E$-07 | 0.23$E$-09 |
| $A\,^2\Sigma^+$ $v=1$ | 2285 | 0.9994 | 0.0003 | 0.0000 | 0.2265$E$-06 | 0.53$E$-10 |
| $A\,^2\Sigma^+$ $v=2$ | 4060 | 0.9989 | 0.0006 | 0.0000 | 0.5429$E$-06 | 0.22$E$-10 |
| $A\,^2\Sigma^+$ $v=3$ | 5780 | 0.9985 | 0.006 | 0.0000 | 0.9671$E$-06 | 0.13$E$-10 |
| $3\,^2\Sigma^+$ $v=0$ | 6863 | 0.0007 | 0.9983 | 0.0055 | 0.2922$E$-07 | 0.41$E$-09 |
| $A\,^2\Sigma^+$ $v=4$ | 7442 | 0.9979 | 0.0009 | 0.0000 | 0.1457$E$-05 | 0.83$E$-11 |
| $1\,^2\Pi$ $v=0$ | 7610 | 0.0000 | 0.0055 | 0.9945 | 0.1575$E$-09 | 0.77$E$-06 |
| $3\,^2\Sigma^+$ $v=1$ | 8665 | 0.0048 | 0.9890 | 0.0061 | 0.4703$E$-07 | 0.26$E$-09 |
| $A\,^2\Sigma^+$ $v=5$ | 9045 | 0.9932 | 0.0015 | 0.0002 | 0.1950$E$-05 | 0.62$E$-11 |
| $1\,^2\Pi$ $v=1$ | 9348 | 0.0001 | 0.0062 | 0.9937 | 0.1376$E$-10 | 0.88$E$-06 |
| $A\,^2\Sigma^+$ $v=6$ | 10 586 | 0.9896 | 0.0084 | 0.0001 | 0.2601$E$-05 | 0.47$E$-11 |
| $3\,^2\Sigma^+$ $v=2$ | 10 416 | 0.0008 | 0.9943 | 0.0049 | 0.1347$E$-09 | 0.90$E$-07 |
| $1\,^2\Pi$ $v=2$ | 11 028 | 0.0000 | 0.0070 | 0.9930 | 0.6167$E$-09 | 0.20$E$-08 |
| $A\,^2\Sigma^+$ $v=7$ | 12 060 | 0.8840 | 0.1132 | 0.0008 | 0.3815$E$-05 | 0.32$E$-11 |
| $3\,^2\Sigma^+$ $v=3$ | 12 105 | 0.1108 | 0.8814 | 0.0074 | 0.1313$E$-09 | 0.92$E$-07 |
| $1\,^2\Pi$ $v=3$ | 12 651 | 0.0000 | 0.0081 | 0.9918 | 0.5789$E$-08 | 0.21$E$-08 |
| $A\,^2\Sigma^+$ $v=8$ | 13 469 | 0.9469 | 0.0503 | 0.0002 | 0.5548$E$-05 | 0.22$E$-11 |
| $3\,^2\Sigma^+$ $v=4$ | 13 735 | 0.0485 | 0.9420 | 0.0093 | 0.1058$E$-05 | 0.11$E$-10 |
| $1\,^2\Pi$ $v=4$ | 14 219 | 0.0002 | 0.0093 | 0.9906 | 0.3132$E$-07 | 0.39$E$-09 |

[a]Energy given with respect $-18.574\,695$ hartree.

2.7 bohr, which is near $R_{\min}$ of the Rydberg states, are in excellent agreement with reported experimental data for *ns*, *np*, and *nd* Rydberg states of KrD.[8–10] There is only one disagreement with the experimental work and this is with regard to the assignment of the $6s$ and $7s$ $^2\Sigma^+$ and the $4d$ and $5d$ $^2\Sigma^+$ levels. The present quantum defect calculations, based on the $s$ character calculated for the $A\,^2\Sigma^+$ state of KrH lead to an $s\leftrightarrow d$ reassignment of the observed $s\,^2\Sigma^+$ and $d\,^2\Sigma^+$ levels.[9,10]

The results of the four-state complex coordinate calculations involving the ground and the first three excited electronic states of KrH (and KrD) yields large predissociation widths for the $^2\Sigma^+$ states in KrH but smaller by a factor of 60 in KrD, in agreement with experimental observations.[8] Only small mixing is found between the levels of the $3\,^2\Sigma^+$ and the $1\,^2\Pi$ $5p$ states, even for high rotational levels, which does not explain their consideration as a $5p$ complex in KrD.[9] However, the $5p$ states in KrD, unlike the higher *np* states, can be equally well considered as isolated states,[9] and with $5p$ $^2\Pi$ considered as a case (a) state.[10]

Finally, potential energy curves are presented for the ground and excited electronic states of the cation, $KrH^+$. Only the ground state is found to have a substantial minimum while the excited states are either repulsive (the lowest four excied states) or are metastable, with local minima at $R_{\min}$ of the ground state of $KrH^+$.

## ACKNOWLEDGMENT

The authors are grateful to the Deutsche Forschungsgemeinschaft for financial support during the course of this work.

[1] I. Martin, C. Lavin, Y. Perez-Delgado, J. Pitarch-Ruiz, and J. Sanchez-Marin, J. Phys. Chem. A **105**, 9637 (2001).
[2] P. G. Alcheev, V. E. Chernov, and B. A. Zon, J. Mol. Spectrosc. **211**, 71 (2002).
[3] J. W. C. Johns, J. Mol. Spectrosc. **36**, 488 (1970).
[4] G. Theodorakopoulos, S. C. Farantos, R. J. Buenker, and S. D. Peyerimhoff, J. Phys. B **17**, 1453 (1984).
[5] G. Herzberg, Annu. Rev. Phys. Chem. **38**, 27 (1987).
[6] G. Theodorakopoulos and I. D. Petsalakis, Chem. Phys. Lett. **149**, 196 (1988).
[7] T. Möller, M. Beland, and G. Zimmerer, Phys. Rev. Lett. **55**, 2145 (1985); Chem. Phys. Lett. **136**, 551 (1987).
[8] I. Dabrowski, G. Herzberg, B. P. Hurley, R. H. Lipson, M. Vervloet, and D.-C. Wang, Mol. Phys. **63**, 269 (1988).
[9] I. Dabrowski and D. A. Sadovskii, Mol. Phys. **81**, 291 (1994).
[10] I. Dabrowski and D. A. Sadovskii, J. Chem. Phys. **107**, 8874 (1997).
[11] I. Dabrowski, D. W. Tokaryk, and J. K. G. Watson, J. Mol. Spectrosc. **189**, 95 (1998).
[12] J. K. G. Watson, Mol. Phys. **81**, 277 (1994).
[13] Ch. Jungen and A. L. Roche, J. Chem. Phys. **110**, 10784 (1999).
[14] I. D. Petsalakis, G. Theodorakopoulos, Y. Li, G. Hirsch, and R. J. Buenker, and M. S. Child, J. Chem. Phys. **108**, 7607 (1998).
[15] Ch. Jungen, A. L. Roche, and M. Arif, Philos. Trans. R. Soc. London, Ser. A **355**, 1481 (1997).
[16] G. Theodorakopoulos, I. D. Petsalakis, and R. J. Buenker, Mol. Phys. **71**, 1055 (1990).
[17] I. D. Petsalakis, G. Theodorakopoulos, and S. Consta, Mol. Phys. **75**, 805 (1992).
[18] I. D. Petsalakis and G. Theodorakopoulos, J. Phys. B **27**, 4483 (1994).
[19] M. Creuzburg and J. Eberlein, Chem. Phys. Lett. **285**, 379 (1988); M. Creuzburg and F. Wittl, J. Lumin. **48/49**, 611 (1991); M. Creuzburg and F. Wittl, J. Mol. Struct. **222**, 127 (1990).
[20] J. Eloranda and H. Kunttu, J. Chem. Phys. **113**, 7446 (2000).
[21] R. J. Buenker, in *Studies in Physical and Theoretical Chemistry, Current Aspects of Quantum Chemistry*, edited by R. Carbo (Elsevier, Amsterdam, 1981), Vol. 2, p. 17.
[22] R. J. Buenker and R. A. Phillips, J. Mol. Struct.: THEOCHEM **123**, 291 (1985).
[23] R. J. Buenker, and S. Krebs, in *Recent Advances in Multireference Methods*, edited by K. Hirao (World Scientific, Singapore, 1999), p. 1.
[24] I. D. Petsalakis, J. Chem. Phys. **110**, 10730 (1999).
[25] M. Molski, Mol. Phys. **100**, 3545 (2002).
[26] H. Hotop, T. E. Roth, M.-W. Ruf, and A. J. Yencha, Theor. Chem. Acc. **100**, 36 (1998).
[27] P. Rosmus and E. A. Reinsch, Z. Naturforsch. A **35**, 1066 (1980).
[28] J. W. C. Johns, J. Mol. Spectrosc. **106**, 124 (1984).
[29] M. M. Hurley, L. F. Pacios, P. A. Christiansen, R. B. Ross, and W. C. Ermler, J. Chem. Phys. **84**, 6840 (1986).

Downloaded 08 Dec 2008 to 194.177.215.121. Redistribution subject to AIP license or copyright; see http://jcp.aip.org/jcp/copyright.jsp

[30] S. Huzinaga, J. Chem. Phys. **42**, 1293 (1969).
[31] S. R. Langhoff and E. R. Davidson, Int. J. Quantum Chem. **8**, 61 (1974).
[32] G. Hirsch, P. J. Bruna, R. J. Buenker, and S. D. Peyerimhoff, Chem. Phys. **45**, 335 (1980).
[33] I. D. Petsalakis, G. Theodorakopoulos, and R. J. Buenker, J. Chem. Phys. **92**, 4920 (1990).
[34] G. Theodorakopoulos and I. D. Petsalakis, J. Chem. Phys. **101**, 194 (1994).
[35] I. D. Petsalakis, G. Theodorakopoulos, and M. S. Child, J. Phys. B **28**, 5179 (1995).
[36] Y. Li, O. Bludsky, G. Hirsch, and R. J. Buenker, J. Chem. Phys. **107**, 3014 (1998).

Downloaded 08 Dec 2008 to 194.177.215.121. Redistribution subject to AIP license or copyright; see http://jcp.aip.org/jcp/copyright.jsp